
PHYSICAL CHEMISTRY
OF WATER TREATMENT PROCESSES

Removal of Fluoride from Aqueous Solution using Calcium Peroxide as a Low-Cost Adsorbent

Parwathi Pillai^a, Swapnil Dharaskar^{a, *, **}, and Hitesh Panchal^b

^aNano-research Group, Department of Chemical Engineering, School of Technology Pandit Deendayal Petroleum University, Gandhinagar, India

^bDepartment of Mechanical Engineering, Government Engineering College, Patan, Gujarat, India

*e-mail: swapnil.dharaskar@sot.pdpu.ac.in

**e-mail: swapnildharaskar11@gmail.com

Received December 5, 2018; revised May 3, 2019; accepted June 14, 2020

Abstract—Removal of fluorides from water is essential for humans and animals because it causes dental and bone deficiency. The maximum permissible limit of fluoride is 1.5 mg/L, according to the World Health Organization. Recently it became known that countries like Pakistan, India, Sri Lanka, China, Argentina, etc. have high fluoride concentration in groundwater. In the present work, calcium peroxide nanoparticles adsorption behaviour and its fluoride removal efficiency from an aqueous phase was studied. Adsorption technique was used to concentrate fluoride on the adsorbent. The advantage of using adsorption is that it is a technique which is easy to implement and relatively cheap. To characterise the structure, size and morphology of adsorbent nanoparticles, Fourier-transform infrared spectroscopy, X-ray powder diffraction, scanning electron microscopy with energy dispersion X-ray spectroscopy, and Raman spectroscopy were applied. In batch adsorption experiments, the process parameters varied were: pH (2–12); contact time (5–60 min); adsorbent dosage (0.05–1 g); concentration (10–100 mg/L), and temperature (5–60°C). The kinetic study has shown that the experimental data are consistent with pseudo second order model with the regression coefficient of 0.99. The adsorption equilibrium is best describable by Langmuir isotherm model with adsorption capacity of 89.6 mg/g. The process thermodynamic was also studied to confirm the proposed mechanism of fluoride adsorption on the adsorbent. The isothermal multistage adsorption was investigated to understand the mechanism of calcium peroxide nanoparticle adsorption for fluoride removal. The maximum fluoride adsorption capacity calculated for CaO₂ was 89 mg/g, with 90% defluoridation efficiency. The results suggested that calcium peroxide nanoparticles can be considered as a promising adsorbent for fluoride removal.

Keywords: adsorption, fluoride, nanoparticles, calcium peroxide

DOI: 10.3103/S1063455X20050082

INTRODUCTION

Fluoride pollutants in drinking water attract great attention worldwide due to their hazards towards humans, such as dental problems, bone deficiency, cancer, thyroid, brain damage, etc [1]. According to World Health Organization, the maximum permissible concentration of fluoride in drinking water is 1.5 mg/L; at the same time, more than 250 million people consume drinking water which has fluoride concentration above this value. Recently, countries like Sri Lanka, Pakistan, India, China, Argentina etc. have high fluoride concentration in ground water [2]. Therefore, the development of new cost-efficient technologies aimed at the removal of fluoride from ground water to minimize the risk to living organisms is a challenge for the foreseeable future.

There exist several technologies for defluoridation, such as adsorption, precipitation, ion-exchange, electrocoagulation, electrodialysis, reverse osmosis and membrane filtration [3]. Among all these, adsorption methods are considered as most promising ones, due to their efficiency and cost-saving nature with respect both to operation and maintenance. Also, nanomaterials and nanotechnologies have done a revolutionized change throughout all field of invention [4]. Nanoparticles (NPs) are very efficient, in particular in the field of adsorption, because of their high surface area and small size. Most materials exhibit better performance in neutral pH but are unstable at high pH values, so it is necessary to adjust pH in industrial and in ground fluoride water [5].

In numerous studies various adsorbents were successfully applied for fluoride removal, such as iron oxide, clay, quick lime, activated carbon, hydroxyapatite, hydrated cement, brick powder, chitosan, metal oxides, red mud, alum impregnated activated alumina, zirconium and zirconium impregnated collagen fiber. Nanoparticles of calcium peroxide (CaO_2) were proposed for arsenic removal, for toluene removal from petroleum products, for the removal of α -toluic acid, for treatment of industrial waste water, etc [6–8].

CaO_2 has the most advantages of larger surface area which enhances the speed of reaction and ensures low process cost. In the current research, CaO_2 NPs were synthesized using coprecipitation method and used as an adsorbent for fluoride removal. NPs were characterized using FTIR, XRD, and SEM/EDX. Efficiency of fluoride removal has been studied at varied values of different parameters such as contact time, temperature, pH, adsorbent dose, initial concentration of fluoride and agitation speed. Kinetic model, thermodynamics and isotherm characteristics were estimated to reveal the adsorption rate and maximum adsorption capacity. To access possible economic benefits, the regeneration studies for the reuse of the adsorbent were also performed.

EXPERIMENTAL

Materials

Calcium chloride (CaCl_2 , 99.5%), ammonia solution ($\text{NH}_3 \cdot \text{H}_2\text{O}$, 25%), polyethylene glycol solution (PEG 200), hydrogen peroxide (H_2O_2 , 35%) were procured from Merck company. All chemicals were used without further treatment and of analytical grade. Deionized water was used for all the experiments.

Preparation Method

CaCl_2 (3 g) was dissolved in deionized water (30 mL) followed by polyethylene glycol (120 mL) and ammonia solution (15 mL). Hydrogen peroxide (H_2O_2) (15 mL) was added at the rate of three drops per minute under constant solution stirring. Subsequently, the solution was stirred for 2 h until it becomes yellowish in color; the pH value of this solution should be 11.5. Afterwards solution was centrifuged at 2000 rpm for 10 min and washed with deionized water twice. Then, NPs were dried in vacuum oven at 90°C for 1 h [6].

Instrumentation

Fluoride measurement was done using Orion star pH/ISE bench-top meter kit Selective Electrode (Orion 720 A⁺ Thermo Scientific). The functional groups present in the adsorbent were detected by FTIR spectrometer. X-ray powder diffraction (XRD) analysis was conducted by X-ray diffractometer (PAN analytical X'pert PRO) using Cu X-ray tube ($\lambda = 1.5406 \text{ \AA}$) to identify the phases present in the NPs. Scanning Electron Microscope (SEM) (Zeiss Ultra 55) was used to characterize the surface morphology, size, and structure of adsorbent. The sample was sputter-coated with a thin film of gold for conductivity for 15 sec. After coating the sample was kept in carbon tape for SEM analysis. For the elemental quantitative analysis, Energy dispersive X-ray spectrometer (EDX) attached to the SEM was used.

Batch Experiments

Fluoride adsorption efficiency was studied in batch experiment using CaO_2 NPs as an adsorbent for various parameters. Each experiment was performed in 100 mL flask of fluoride solution with desired amount of adsorbent kept in orbital shaker. After shaking the solution was centrifuged at 2000 rpm. Later, solution was measured in fluoride meter. The percentage of fluoride removal was calculated using the equation:

$$\%F = \frac{C_0 - C_e}{C_0} \times 100, \quad (1)$$

where C_0 and C_e are the fluoride initial and equilibrium concentrations (g/L), respectively.

RESULTS AND DISCUSSION

Material Characterizations

FTIR analysis was performed to indicate the presence of the functional groups in the CaO₂ NPs adsorbent; the result is shown in Fig. 1a, where the bond formation in the range of 400–4000 cm⁻¹ is evidenced. Stretching of OCaO bond is observed in 550 cm⁻¹ band and the other two peaks which correspond to O–O stretching are present at 715 and 766 cm⁻¹. Moreover, peaks at 873 and 1464 cm⁻¹ show the presence of carbonate and 1795 cm⁻¹ peak indicates the presence of C=O bond. The peak at 3640 cm⁻¹ corresponds to stretching of O–H bond [7].

XRD Analysis

X-ray diffraction patterns analysis was performed to discover the NPs phase of CaO₂ as shown in Fig. 1b. The diffraction pattern exhibits peaks at 2θ values of 30.6°, 35.9°, 47.7°, 51.6°, 53.5° and 60.7° corresponding to characteristic peaks (002), (110), (112), (200), (103) and (202), which indicate the existence of tetragonal phase, in good agreement with the CaO₂ reference pattern (JCPDS-03-0865) [8].

SEM and EDX

The morphology of CaO₂ NPs was studied by SEM with EDX analysis; the results are shown in Fig. 1c. It appears clearly that NPs are spherical in shape while EDX shows the elements C, O, Ca, N, Au present in NPs [9].

Effect of Adsorption Parameters on Fluoride Removal

Influence of adsorbent dose and contact time. Batch experiment study was performed to examine the effects of CaO₂ NPs adsorbent dose on fluoride removal efficiency at pH 7, as shown in Fig. 2a. Fluoride removal increased with the increase of the adsorbent dose from 0.1 to 0.7 g/L, but for higher doses no such rise was observed, that is, the removal remained constant up to 1.0 g/L dose. The maximum removal efficiency thus achieved correspond to the adsorption capacity of 89 mg/g. The plateau of removal efficiency should be ascribed to the unavailability of active sites. Similar trend line was described in the literature [10]. The dependence of fluoride removal efficiency on contact time in batch experiment was studied by keeping the adsorbent dose 0.7 g/L at pH 7; the results are illustrated in Fig. 2b. In batch adsorption, the fluoride acceptance was found to increase until 40 min with 89 mg/L adsorption capacity. After 40 min, adsorption process slows down because of the unavailability of vacant sites. The same results were reported in the literature [11].

Impact of Temperature and Initial Fluoride Concentration on Adsorption Efficiency

To study the effect of temperature and initial fluoride concentration in aqueous solution on the fluoride removal efficiency, batch experiments were performed. The effect of temperature in the range of 5 to 60°C at the adsorbent dose 0.7 g/L, pH 7, contact time 40 min and mixing at 200 rpm was studied. It was noticed that initially with the temperature increase the efficiency also increased, but then decreased at further increase of temperature. This could be explained by the increase of the randomness of fluoride ion motion at higher temperature [12]. The maximum adsorption obtained at 25°C with 89 mg/L adsorption capacity. The same dependence on temperature was reported in literature [13].

The dependence of fluoride adsorption by CaO₂ NPs on its initial concentration was studied at the concentration range of 10 to 100 mg/L at the optimum process parameters: adsorbent dose 0.7 g/L, pH 7, contact time up to 40 min, and mixing at 200 rpm. It was found that the fluoride removal efficiency decreases with the concentration increase. Highest adsorption was observed at 10 mg/L with 89 mg/g adsorption capacity. This trend was reported in literature [14].

Influence of pH

The interaction between fluoride ion and CaO₂ NPs depends on the pH impact. To reveal the mechanism of this interaction, the studies were performed in the pH range of 2 to 12; the results are shown in Fig. 2c. It is seen that the adsorption capacity first increases with pH, and then the decrease occurs above

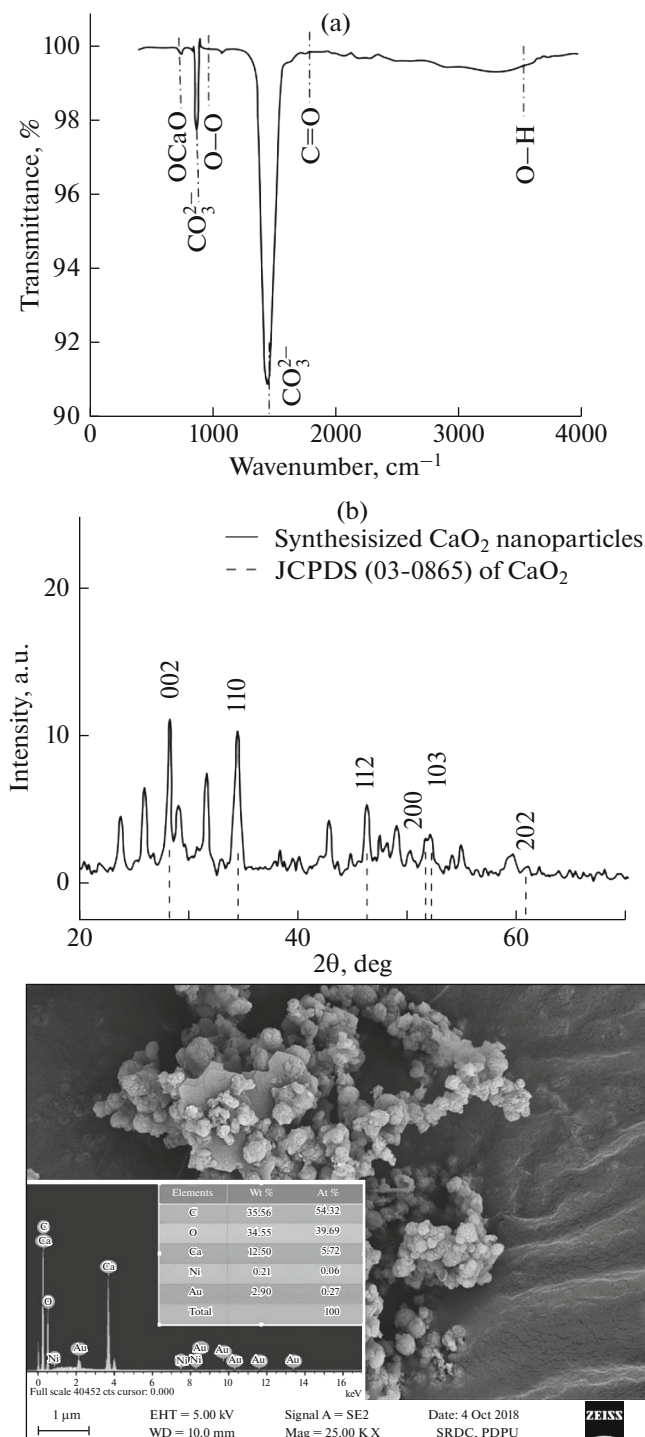


Fig. 1. Characterisation of CaO_2 nanoparticles: (a) FTIR spectra; (b) XRD; (c) SEM-EDX.

certain pH value. In acidic medium, fluoride ions become partly protonated, forming the hydrofluoric acid; this leads to the decrease of adsorption. The pH in alkaline medium the adsorption is lower than that at the neutral pH, because the repulsion exists between the fluoride negative ions and hydroxide ions. Therefore, the optimum pH value using CaO_2 NPs as adsorbent for fluoride removal is 7, with 89 mg/g adsorption capacity. This also had been confirmed when the pH_{pzc} value was determined. The similar pH trend was also described in literature [15].

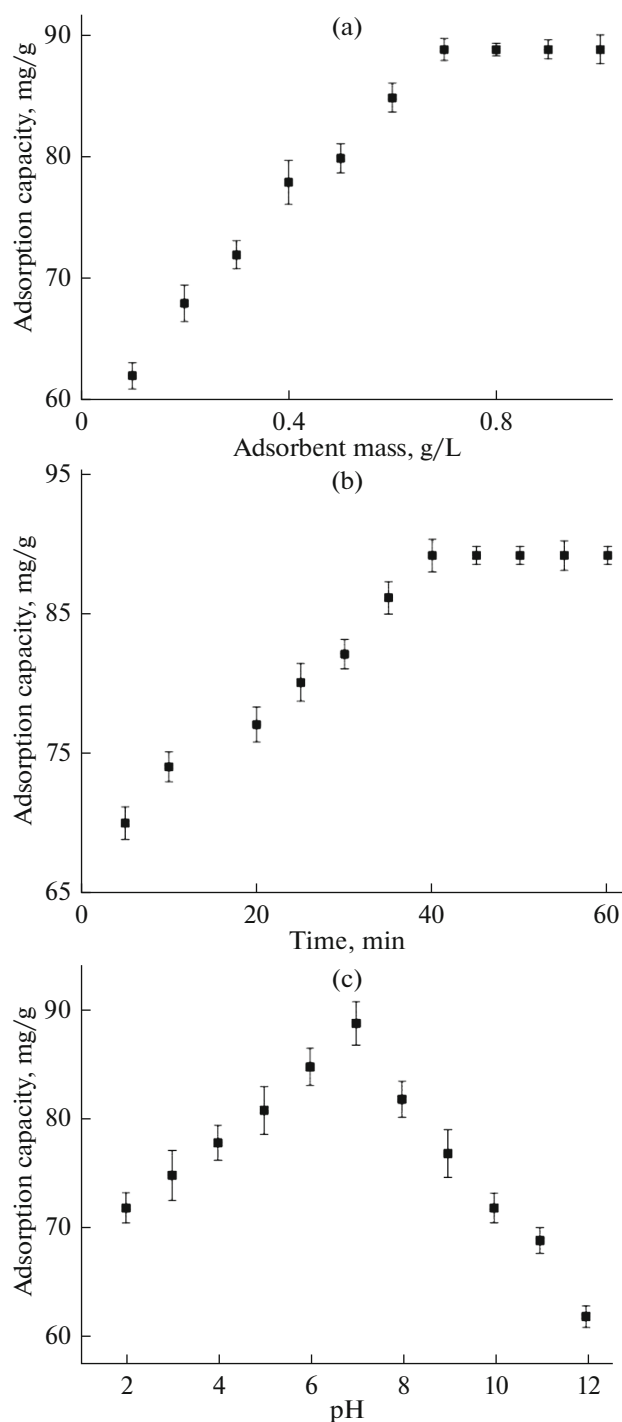


Fig. 2. Dependence of CaO_2 nanoparticles adsorption capacity with respect to fluoride removal: (a) adsorbent dose; (b) contact time; (c) pH.

Adsorption Kinetics, Isotherm and Thermodynamics

The adsorption kinetics study reveals the mechanism of adsorption process. To analyse adsorption kinetics for the fluoride removal using CaO_2 NPs adsorbent, the time dependent pseudo-first order and pseudo-second order models were applied. The kinetic data are shown in Fig. 3a and Table 1. The correspondence of either model to the studied process was based on the regression coefficient R^2 value, and on the agreement between the experimental and calculated values of q_e .

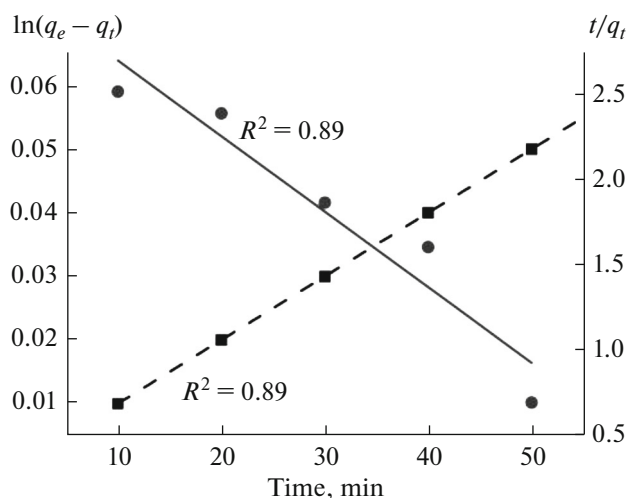


Fig. 3. Graphical estimation of kinetic model type and parameters: (●) pseudo-first order; (■) pseudo-second order.

Pseudo-first order model assumes that the difference in adsorbed amounts per unit sorbent mass between the value at equilibrium q_e and the value at time tq_t is directly proportional to the adsorption rate dq_t/dt , which is expressed by Eq. (2):

$$\ln(q_e - q_t) = \ln q_e - k_1 t. \quad (2)$$

The plot of $\ln(q_e - q_t)$ vs t provides the slope as rate constant k_1 , and intercept as equilibrium adsorption capacity q_e . For this dependence the parameters thus estimated are listed in Table 1, and regression coefficient was found to be 0.89. It was found that the calculated value of equilibrium adsorption capacity $q_{e,calc}$ does not agree with its experimental value $q_{e,exp}$, therefore the pseudo-first order model cannot be applied to describe the adsorption of fluoride by CaO_2 NPs adsorbent, and the process is not diffusion controlled [16].

To analyse the adsorption kinetics using the pseudo-second order model, which is described by the equation [17]:

$$\frac{t}{q_t} = \frac{1}{k_2 q_e^2} + \frac{t}{q_e}, \quad (3)$$

the graphical dependence of t/q_e vs t was plotted, as shown in Fig. 3, which gives the kinetic constant k_2 determined from the slope and equilibrium sorption capacity q_e from the intercept. The values thus obtained are listed in Table 1. The corresponding regression coefficient R_2^2 was found to be 0.99; also, the calculated and experimental values of equilibrium adsorption capacity are in a relatively good mutual correspondence. It could be concluded therefore that the pseudo-second order model provides a better description of the fluoride removal using CaO_2 NPs adsorbent process than the pseudo-first order model.

Adsorption isotherm was used to evaluate the CaO_2 NPs adsorbent efficiency. It gives the information about the reaction viability, adsorbent surface properties, and mechanism which governs the adsorption. In this present work, experimental data were fitted with two isotherms, Langmuir and Freundlich. For the fitting, the experimental data for fluoride adsorption from its aqueous solution with initial concentration 10 mg/L and the CaO_2 NPs adsorbent dose of 0.7 g/L. The adsorption isotherm parameters obtained by the two models are listed in Table 2.

Table 1. Kinetic constants and correlation coefficient for initial fluoride concentration 10 mg/L

| Pseudo-first order kinetic model | | | | Pseudo-second order kinetic model | | |
|----------------------------------|--------------|-------|---------|-----------------------------------|-------|---------|
| $q_{e,exp}$ | $q_{e,calc}$ | k_1 | R_1^2 | $q_{e,calc}$ | k_2 | R_2^2 |
| 2.5 mg/L | 1.11 mg/L | 0.37 | 0.89 | 2.9 mg/L | 1.1 | 0.99 |

Table 2. Langmuir and Freundlich isotherm of CaO₂ nanoparticles for adsorption of fluoride at initial fluoride concentration 10 mg/L

| Langmuir isotherm | | Freundlich isotherm | |
|-------------------|------------|---------------------|-------|
| q_m | 89 mg/g | K_f | 0.764 |
| b | 0.014 mg/L | n | 1.105 |
| R_L^2 | 0.98 | R_F^2 | 0.72 |

Langmuir isotherm assumes that adsorbent active sites are evenly distributed over the surface and only one molecule can be adsorbed at the active site; this mechanism corresponds to monolayer adsorption. It is assumed also that there is no interaction between adsorbed molecules. The equation which describe Langmuir model is [18]:

$$\frac{t}{q_e} = \frac{1}{q_m b C_e} + \frac{1}{q_m}, \quad (4)$$

where q_m is the maximum fluoride adsorption capacity (mg/g), q_e is the equilibrium adsorption capacity (mg/g), b is the adsorption activity coefficient (L/mg) and C_e (mg/L) is the concentration of fluoride at equilibrium in solution. From the plot of $1/q_e$ vs $1/C_e$ shown in Fig. 4 the values q_m and b were estimated; also, the regression coefficient R_L^2 was found to be 0.98 which suggests that Langmuir model could provide a sound description of the fluoride adsorption on CaO₂ nanoparticles with highest adsorption capacity of 89.6 mg/g [20]. On the contrary, Freundlich isotherm model which is described by the equation [19]:

$$\log q_e = \log K_F + \frac{1}{n} \log C_e, \quad (5)$$

where K_F is the measure of adsorption capacity and $1/n$ is the adsorption intensity of heterogeneous system, when fitted to the experimental data, yields the values of coefficients listed in Table 2, and the regression coefficient $R_F^2 = 0.72$ which is essentially worse than that obtained for the Langmuir model. It could be concluded therefore that the fluoride adsorption from its aqueous solution onto the surface of CaO₂ NPs obeys the Langmuir monolayer adsorption model.

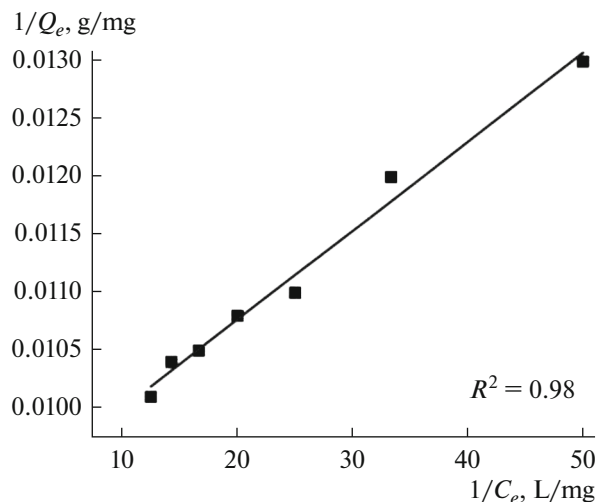
**Fig. 4.** Graphical estimation of Langmuir isotherm parameters.

Table 3. Gibbs' free energy data for initial fluoride concentration 10 mg/L

| ΔH° , kJ/mol | ΔS° , kJ/K/mol | ΔG° , kJ/mol | | | |
|---------------------------|-----------------------------|---------------------------|-------|-------|-------|
| | | 15°C | 25°C | 30°C | 35°C |
| -3.3 | 0.3 | -7.8 | -10.8 | -12.3 | -13.8 |

Process Thermodynamics Study

Adsorption nature and possibility of the process are determined by thermodynamics factors. Therefore, the behaviour of thermodynamic quantities, viz. enthalpy variation ΔH , free energy variation ΔG , and entropy variation ΔS was estimated within the studied temperature range. It was shown above that the fluoride adsorption by CaO_2 NPs was more efficient at moderate temperatures, while the temperature increase results in sharp adsorption decrease, i.e. the interaction of fluoride ion with NPs active centres weakens at higher temperature. The behaviour of the studied system is governed by the electrostatic interaction between fluoride ions and CaO_2 NPs active centres. The fluoride adsorption becomes higher with the decrease of temperature, as shown by the ΔG values calculated at different temperatures. The Gibbs free energy values shown in Table 3 were calculated using and equations (6)–(8) [20]:

$$\Delta G = RT \ln K_c, \quad (6)$$

$$\Delta G = \Delta H - T \Delta S, \quad (7)$$

$$\log \left(\frac{q_e m}{C_e} \right) = \frac{\Delta S^\circ}{2.303R} - \frac{\Delta H^\circ}{2.303RT}, \quad (8)$$

where K_c is the equilibrium constant, R is the universal gas constant, and T is the absolute temperature. From the slope and intercept of the plot of K_c vs $1/T$, the ΔH and ΔS values were determined.

Negative values of adsorption free energy variation indicate the realizability of reaction and spontaneous nature of the process at studied temperatures. During fluoride adsorption the ΔG value decreases with the increase of temperature, which indicates that the reaction becomes less probable. Positive entropy variation value indicates the increase of stochasticity of the interactions at the solution-solid interface, which in turn indicates the increase in degrees of freedom at the CaO_2 NPs and fluoride solution interface [21].

Regeneration and Desorption Study

The efficiency of CaO_2 NPs adsorbent was demonstrated by batch experiments performed in static regime. Separate regeneration cycles were carried out at the conditions chosen as optimal to determine the fluoride adsorption after each cycle. After the fluoride adsorption from its solution of 10 mg/L concentration, the adsorbent was vigorously stirred in NaOH solution for 30 min. Then the adsorbent was separated by centrifugation and dried at 90°C to be further used at the same optimum conditions. The degree of desorption and subsequent adsorption was 82–95%. The efficiency of fluoride removal up to 6th regeneration cycle was 82%. After 6th cycle the fluoride mass per unit adsorbent mass was 12.08 mg/g while after the first cycle the value was 24.2 mg/g. The results of the studies visualised in Fig. 5, indicate the CaO_2 NPs adsorbent reusability for the removal of fluoride from aqueous solution [22].

Probable Mechanism of Fluoride Adsorption

The mechanism of fluoride ion adsorption on CaO_2 NPs is probably as follows. The binding of CaO_2 and fluoride ion can exist due to the electrostatic attraction. Moreover, the bond of C=O and the ion pair attraction with the F^- ion can contribute to the adsorption, which accelerates the adsorption process and enhance the fluoride removal with CaO_2 NPs.

CONCLUSIONS

In the present work, CaO_2 NPs were synthesized at room temperature. The structure, size, crystallography and morphology of the adsorbent were confirmed by FTIR, XRD and SEM/EDX. The maximum adsorption capacity with respect to fluoride was above 89 mg/L, which was attained within 40 min of adsorption at 25°C, adsorbent dosage 0.7 g/L, pH 7 and fluoride concentration in aqueous solution

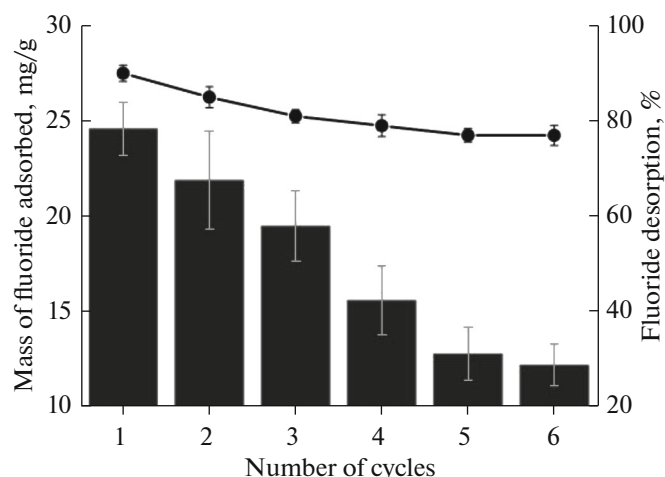


Fig. 5. Estimation of sorbent regeneration properties: bars, fluoride adsorbed amount; points, fluoride desorption efficiency, as dependent on the number of regeneration cycles.

10 mg/L. The percentage of adsorption decreased gradually with increase in initial fluoride concentration. The results of the adsorption equilibrium studies show that fluoride adsorption on CaO_2 NPs obeys Langmuir isotherm with an adsorption capacity of 89.6 mg/g, indicating the monolayer adsorption on the NPs surface. The estimation of thermodynamic parameters of adsorption (estimated ΔH° value -3.3 kJ/mol) suggests that the adsorption is spontaneous and exothermic in nature, and further confirms the physico-chemical mechanism of adsorption process of fluoride. Regeneration studies have shown that the adsorbent can be reused up to 6th cycle with good adsorption efficiency. To summarise, this study demonstrated that the synthesized adsorbent may be considered as promising for fluoride removal from aqueous solution.

ACKNOWLEDGMENTS

Authors gratefully acknowledge the Solar Research and Development Center (SRDC), School of Technology, Pandit Deendayal Petroleum University, Raisan, Gujarat, India for the support in the characterization analysis.

REFERENCES

- Pandya, J.B., Mehta, K.J., and Patale, V.V., Study of fluoride content in ground water from villages of Patan Taluka of Gujarat, India, *J. Ind. Pollut. Control.*, 2012, vol. 28, pp. 161–164.
- Bandewar, S., Mane, S., and Tirthakar, S., Removal of fluoride from drinking water by using low cost adsorbent, *Int. J. Res. Eng. Technol.*, 2015, vol. 4, pp. 349–351.
- Pillai, P., Dharaskar, S., Sasikumar, S., and Khalid, M., Zeolitic imidazolate framework-8 nanoparticle: A promising adsorbent for effective fluoride removal from aqueous solution, *Appl. Water Sci.*, 2019, vol. 9, pp. 1–12.
- Pillai, P., Lakhtaria, Y., Dharaskar, S., and Khalid, M., Synthesis, characterization, and application of iron oxyhydroxide coated with rice husk for fluoride removal from aqueous media, *Environ. Sci. Pollut. Res.*, 2020, vol. 27, pp. 20606–20620.
- Mohapatra, M., Hariprasad, D., Mohapatra, L., Anand, S., and Mishra, B.K., Mg-doped nano ferrihydrite—A new adsorbent for fluoride removal from aqueous solutions, *Appl. Surf. Sci.*, 2012, vol. 258, pp. 4228–4236.
- Madan, S.S., Wasewar, K.L., and Pandharipande, S.L., Modeling the adsorption of benzeneacetic acid on CaO_2 nanoparticles using artificial neural network, *Resour. Technol.*, 2016, vol. 2, pp. 53–62.
- Yeh, C.S., Wang, R., Chang, W.C., and Shih, Y-H., Synthesis and characterization of stabilized oxygen-releasing CaO_2 nanoparticles for bioremediation, *J. Environ. Manage.*, 2018, vol. 212, pp. 17–22.
- Madan, S.S., Wasewar, K.L., and Ravi Kumar, C., Adsorption kinetics, thermodynamics, and equilibrium of α -toluic acid onto calcium peroxide nanoparticles, *Adv. Powder Technol.*, 2016, vol. 27, pp. 2112–2120.
- Guo, Z.Q., Miao, N.X., Zhou, J.P., Lei, Y.X., Hassan, Q.U., and Zhou, M.M., Novel magnetic semiconductor $\text{Na}_2\text{Fe}_2\text{Ti}_6\text{O}_{16}$: Synthesis, double absorption and strong adsorptive ability, *J. Mater. Chem.*, 2017, vol. 5, pp. 17589–17600.

10. Wu, X., Zhang, Y., Dou, X., and Yang, M., Fluoride removal performance of a novel Fe–Al–Ce trimetal oxide adsorbent, *Chemosphere*, 2007, vol. 69, pp. 1758–1764.
11. Bibi, S., Farooqi, A., Hussain, K., and Haider, N., Evaluation of industrial based adsorbents for simultaneous removal of arsenic and fluoride from drinking water, *J. Clean. Prod.*, 2015, vol. 87, pp. 882–896.
12. Ho, Y.S. and McKay, G., The kinetics of sorption of basic dyes from aqueous solution by sphagnum moss peat, *Can. J. Chem. Eng.*, 1998, vol. 76, pp. 822–827.
13. Sharma, S. and Kennedy, M., Development of iron oxide nanoparticle adsorbents for arsenic and fluoride removal, *Desalin. Water Treat.*, 2017, vol. 67, pp. 187–196.
14. Li, Y.H., Wang, S., Cao, A., Zhao, D., Zhang, X., Xu, C., Luan, Z., Ruan, D., Liang, J., Wu, D., and Wei, B., Adsorption of fluoride from water by amorphous alumina supported on carbon nanotubes, *Chem. Phys. Lett.*, 2001, vol. 350, pp. 412–416.
15. Dey, A., Singh, R., and Purkait, M.K., Cobalt ferrite nanoparticles aggregated schwertmannite: A novel adsorbent for the efficient removal of arsenic, *J. Water Process Eng.*, 2014, vol. 3, pp. 1–9.
16. Zhang, C., Li, Y., Jiang, Y., and Wang, T.-J., Size-dependent fluoride removal performance of a magnetic Fe₃O₄Fe–Ti adsorbent and its defluoridation in a fluidized bed, *Ind. Eng. Chem. Res.*, 2017, vol. 56, pp. 2425–2432.
17. Lu, J.-F. and Tsai, C.-J., Hydrothermal phase transformation of hematite to magnetite, *Nanoscale Res. Lett.*, 2014, vol. 9, pp. 1–8.
18. Rajkumar, S., Muruges, S., Sivasankar, V., Darchen, A., Msagati, T.A.M., and Chaabane, T., Low-cost fluoride adsorbents prepared from a renewable biowaste: Syntheses, characterization and modeling studies, *Arab. J. Chem.*, 2019, vol. 12, pp. 3004–3017.
19. Medellin-Castillo, N.A., Leyva-Ramos, R., Padilla-Ortega, E., Perez, R.O., Flores-Cano, J.V., and Berber-Mendoza, M.S., Adsorption capacity of bone char for removing fluoride from water solution. Role of hydroxyapatite content, adsorption mechanism and competing anions, *J. Ind. Eng. Chem.*, 2014, vol. 20, pp. 4014–4021.
20. Bhaumik, M., Leswif, T.Y., Maity, A., Srinivasu, V.V., and Onyango, M.S., Removal of fluoride from aqueous solution by polypyrrole/Fe₃O₄ magnetic nanocomposite, *J. Hazard. Mater.*, 2011, vol. 186, pp. 150–159.
21. Gangadhar, G., Maheshwari, U., and Gupta, S., Application of nanomaterials for the removal of pollutants from effluent streams, *Nanosci. Nanotechnol.*, 2012, vol. 2, pp. 140–150.
22. Srivastava, V.C., Mall, I.D., and Mishra, I.M., Optimization of parameters for adsorption of metal ions onto rice husk ash using Taguchi's experimental design methodology, *Chem. Eng. J.*, 2008, vol. 140, pp. 136–144.